THE BELL SYSTEM TECHNICAL JOURNAL
Vol. 51, No. 6, July-August, 1972
Printed in U.S.A.

Pulse Propagation in Multimode Dielectric Waveguides

By D. MARCUSE

(Manuscript received November 4, 1971)

Using coupled power equations to describe the average performance of a multimode waveguide with random coupling, it is shown that a Gaussian input pulse remains approximately Gaussian with a pulse width that increases proportionally to the square root of the length of the waveguide. The proportionality factor is determined for the model of a slab waveguide. Since coupling between guided modes of necessity causes coupling of some of the guided modes to radiation modes, radiation losses are unavoidable. A desired improvement in pulse distortion that is accomplished by coupling the guided modes intentionally to each other must be paid for by a certain loss penalty. This loss penalty is also evaluated for the special case of the slab waveguide model. Pulse dispersion improvement can be achieved by providing intentional roughness of the core-cladding interface of the dielectric waveguide. The "power spectrum" of the core-cladding interface function must be designed very carefully in order to minimize the radiation loss penalty that accompanies any attempt to reduce pulse dispersion. The dependence of the loss penalty on the shape of the "power spectrum" of the core-cladding interface function is studied in this paper. Design criteria for the improvement of multimode pulse dispersion are given based on the slab waveguide model. The connection between the slab waveguide model and the round optical fiber is pointed out.

I. INTRODUCTION

S. D. Personick[1] was the first to realize that coupling between the guided modes of a multimode waveguide is capable of reducing the pulse dispersion that is caused by the fact that modes with higher group velocity arrive at the receiver earlier than modes with lower group velocity. Multimode pulse dispersion can, of course, be avoided by designing the waveguide to operate with only a single mode. However, single-mode waveguides cannot be excited efficiently by incoherent

light sources such as luminescent diodes. A simple communications system using luminescent diodes instead of more expensive lasers as light sources needs multimode optical waveguides as the transmission medium. Unless multimode pulse dispersion can be reduced by some means, the information-carrying capacity of a multimode optical fiber is severely limited. Even though Personick[1] pointed the way for achieving an improvement in the multimode pulse dispersion he did not give design criteria for their construction nor did he discuss the loss penalty that inevitably must be paid for any improvement in pulse dispersion. Furthermore, Personick's paper deals primarily with two modes even though some thought is given to the multimode case. H. E. Rowe and D. T. Young[2] rederived Personick's results using a more rigorous analysis but also limited themselves to the two-mode case. Patent applications by E. A. J. Marcatili, S. E. Miller, and S. D. Personick are pending. These patents describe the geometry of a fiber designed to improve multimode pulse distortion by means of mode coupling.

The theory presented in this paper is applicable to an arbitrary number of modes. Utilizing coupled equations (derived in an earlier paper[3]) for the average power carried by the modes of the guide and extending the discussion of the steady state multimode waveguide to the time varying case, a complete description of pulse propagation in multimode waveguides is formally set forth. This complete theory can be evaluated only approximately by means of perturbation theory. Using a second-order perturbation approach a solution of the pulse problem is presented with the assumption that the input pulse has a Gaussian shape (in time). Numerical evaluation of the theory requires matrix diagonalization that can be accomplished on a high-speed electronic computer. The theory is applied to the dielectric slab waveguide; and design criteria for this case are obtained. However, we also extrapolate the slab waveguide results to the more interesting case of the round optical fiber.

The coupling coefficients used in this paper are derived from a first-order perturbation theory. Therefore, they hold only for weak coupling. In case of strong coupling, the actual radiation losses are expected to be larger than predicted here.

II. DISCUSSION OF THE PRINCIPLE OF PULSE DISTORTION REDUCTION

S. D. Personick[1] discovered that coupling between the guided modes of a multimode waveguide with a random coupling function reduces the spread of a pulse whose power is shared by a large number of modes

traveling with slightly different group velocities. Dielectric waveguides have two types of modes. The guided modes that are capable of transporting power through the waveguide and radiation modes that allow the description of the radiation field around the waveguide. Imperfections in the waveguide that couple the guided modes among each other also tend to couple the guided modes to the radiation field. The coupling of guided modes to each other and to radiation modes is well understood.[4,5] In particular it is known that–to first order–two guided modes couple only by means of one component of the Fourier spectrum of the coupling function.[4,6] Figure 1 shows a schematic plot of the possible propagation constants β of the modes of a dielectric slab waveguide. Also shown is a bracket connecting two guided modes. The separation of these modes is

$$\Delta\beta = \beta_\nu - \beta_\mu . \tag{1}$$

The coupling function can be represented as the product of a constant term times a function of z, the distance along the waveguide axis.[7]

$$c_{\nu\mu}(z) = K_{\nu\mu} f(z). \tag{2}$$

The function f can be expanded in a Fourier series[4]

$$f(x) = \sum_{n=-\infty}^{\infty} a_n e^{i\phi_n x} \tag{3}$$

with

$$\phi_n = \frac{2\pi}{z} n. \tag{4}$$

The two guided modes ν and μ are coupled only by the Fourier com-

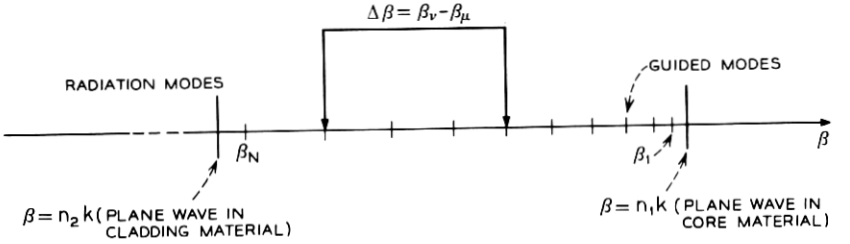

Fig. 1—Schematic representation of the propagation constants β_ν of the guided modes. $n_1 k$ is the propagation constant of plane waves in the core material, $n_2 k$ is the plane wave propagation constant in the cladding material. The line labeled $\Delta\beta$ indicates two guided modes that are coupled by a sinusoidal core-cladding interface irregularity of mechanical frequency $\Delta\beta$.

ponent whose mechanical frequency is given by

$$\phi_n = \beta_\nu - \beta_\mu . \tag{5}$$

If no Fourier component at this mechanical frequency exists the modes remain uncoupled. In order to couple all the guided modes shown in Fig. 1 to each other, we need a Fourier spectrum that has components at all those mechanical frequencies that correspond to existing differences $\beta_\nu - \beta_\mu$. However, in addition to coupling the guided modes among each other, the coupling mechanism also couples guided modes to radiation modes. The coupling law remains the same. Any Fourier component that has a mechanical frequency in the range[6]

$$\beta_\nu - n_2 k \leqq \phi_n \leqq \beta_\nu + n_2 k \tag{6}$$

($n_2 k$ is the propagation constant of plane waves in the medium of the cladding material) couples the mode ν to the radiation field. Coupling between guided modes and radiation modes results in radiation loss. It is thus apparent that we must avoid coupling guided modes to radiation modes or at least try to couple as few of the guided modes as possible to the radiation field without destroying the coupling between the guided modes. It is apparent from Fig. 1 that it is possible to couple all the guided modes among each other and couple only the highest-order guided mode to the radiation field. This selective coupling is made possible by the fact that the spacing between guided modes in β space decreases with decreasing mode number. Ideally we would want a "power spectrum" $F(\phi)$ of the function $f(z)$ as shown in Fig. 2. This spectrum is flat from zero mechanical frequencies to the maximum frequency $\phi_{max} = \beta_{N-2} - \beta_{N-1}$ that is chosen to be equal to the separation between the modes $N - 2$ and $N - 1$. The last guided mode, N, is close to the radiation field so that the Fourier spectrum of the func-

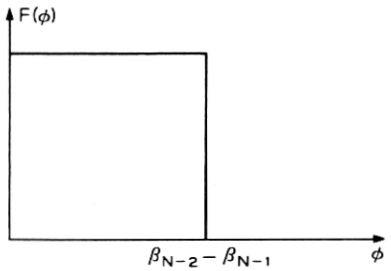

Fig. 2—Ideal shape of the "power spectrum" of the core-cladding interface irregularities.

tion $f(z)$ shown in Fig. 2 couples this mode strongly to the radiation field without coupling it to mode $N - 1$ or any other of the guided modes. The high-order modes are coupled only to their next neighbor while more than two low-order guided modes couple directly to each other because of their close spacing. It would be more efficient for the purposes of pulse distortion reduction to couple each guided mode individually to all the other guided modes. However, since it is impossible to accomplish this without simultaneously coupling all the guided modes directly to radiation modes we must be content to try to couple each guided mode at least to its nearest neighbor. The mechanical "power spectrum" of Fig. 2 would accomplish pulse distortion reduction by means of coupling between the guided modes without any radiation loss penalty. The reduction in the pulse length compared to the uncoupled case comes about because some of the power traveling in a fast mode is eventually transferred to a slow mode while power starting out in a slow mode finds itself at least partly in a fast mode so that the extremes of the group velocity spread are partly equalized causing the center of gravity of the pulse distribution to travel at an average velocity.

The perfect pulse distortion reduction scheme just outlined cannot be realized in practice since it is impossible to build filters with infinitely steep slopes. We can imagine that it is possible to produce a mechanical spectrum of core-cladding interface irregularities by changing the pulling speed of the fiber as it is drawn from the melt or from a preform. If the speed modulation is derived from an electrical noise signal that is filtered by a low-pass filter the problem is reduced to designing an electrical filter with as steep a slope as possible. More details of the required slope will be discussed later when we study the results of the numerical analysis of pulse propagation in slab waveguides.

III. THEORY OF PULSE PROPAGATION IN MULTIMODE WAVEGUIDES

It was shown in an earlier paper[3] how, starting from coupled wave equations, it is possible to obtain stochastic equations for the average power P_ν carried by N modes. In the steady state case discussed in Refs. 3 and 7 the coupled power equations assume the form

$$\frac{dP_\nu}{dz} = -(\alpha_\nu + b_\nu)P_\nu + \sum_{\mu=1}^{N} h_{\nu\mu}P_\mu \tag{7}$$

with

$$b_\nu = \sum_{\mu=1}^{N} h_{\nu\mu} \, . \tag{8}$$

The form of the symmetric matrix elements (power coupling coefficients) $h_{\nu\mu}$ depends on the type of waveguide and the particular coupling mechanism that is being considered, α_ν is the power loss coefficient that results from the coupling of mode ν directly to the radiation field.

Our first task is to generalize the steady state equation (7) to the time-dependent case. This generalization is achieved by considering a moving observer traveling at the group velocity v_ν of one of the guided modes. Whereas a stationary observer sees the average power in this mode grow or diminish as a function of z without noticing any change in time (in the steady state), the moving observer sees the mode power grow in time. The derivative dP_ν/dz noticed by the stationary observer corresponds to the derivative $(1/v_\nu)dP_\nu/dt$ observed in a coordinate system traveling at velocity v_ν . We can thus write for the steady-state case

$$\frac{dP_\nu}{dz} = \frac{1}{v_\nu}\frac{dP_\nu}{dt}. \tag{9}$$

The extension to the time-varying case consists in using the right-hand side of (9) even if the stationary observer sees the mode field change in time. This extension is certainly plausible if the time variations are not too rapid. Keeping in mind that the total time derivative corresponds to the change seen by the moving observer, we introduce the space- and time-dependent functions $P_\nu(z, t)$ and write

$$\frac{dP_\nu}{dt} = \frac{\partial P_\nu}{\partial t} + \frac{\partial P_\nu}{\partial z}\frac{dz}{dt} = v_\nu\frac{\partial P_\nu}{\partial z} + \frac{\partial P_\nu}{\partial t}. \tag{10}$$

The partial derivatives on the right-hand side of (10) are again the changes that are seen by a stationary observer. The time-dependent coupled power equations can thus be written as

$$\frac{\partial P_\nu}{\partial z} + \frac{1}{v_\nu}\frac{\partial P_\nu}{\partial t} = -(\alpha_\nu + b_\nu)P_\nu + \sum_{\mu=1}^{N} h_{\nu\mu}P_\mu . \tag{11}$$

Equation (11) is the starting point for the study of pulse propagation in multimode dielectric waveguides.

We obtain a formal solution of the time-dependent problem by substitution of the trial solution

$$P_\nu(z, t) = B_\nu e^{-\alpha z + i\omega t}. \tag{12}$$

The parameter ω would usually be considered to be the frequency of the time-dependent process (12). However, the average power P_ν is not sinusoidally time-varying so that it cannot be associated with a frequency. The parameter ω is thus simply a variable of integration for a Fourier integral expansion of the function $P_\nu(z, t)$. Substitution of (12)

into (11) leads to the following algebraic eigenvalue problem for the eigenvalue α and the eigenvector B_ν (B_ν is the νth element of an N dimensional vector):

$$\left[-\alpha + i\frac{\omega}{v_o} + i\omega\left(\frac{1}{v_\nu} - \frac{1}{v_o}\right)\right]B_\nu = -(\alpha_\nu + b_\nu)B_\nu + \sum_{\mu=1}^{N} h_{\nu\mu}B_\mu \,. \tag{13}$$

The term with the average group velocity v_o was added for reasons that will become clear shortly. This eigenvalue problem has N solutions. The complete solution of (11) is obtained as a linear superposition of the N eigensolutions plus an integration over the parameter ω:

$$P_\nu(z, t) = \sum_{j=1}^{N} \int_{-\infty}^{\infty} c_j(\omega)B_\nu^{(j)}(\omega)e^{-\alpha^{(j)}(\omega)z}e^{i\omega t}\, d\omega. \tag{14}$$

The superscript j was attached to label the eigenvalues $\alpha(\omega)$ and the eigenvectors $B_\nu(\omega)$. Using the orthogonality of the eigenvectors $B_\nu(\omega)$ of the symmetric real matrix defined by (13),

$$\sum_{\nu=1}^{N} B_\nu^{(i)}B_\nu^{(j)} = \delta_{ij} \,, \tag{15}$$

and the inversion of the Fourier integral allows us immediately to express the expansion coefficient in terms of the power distribution $P_\nu(0, t)$ at the input of the waveguide.

$$c_i(\omega) = \frac{1}{2\pi}\sum_{\nu=1}^{N} \int_{-\infty}^{\infty} B_\nu^{(i)}(\omega)P_\nu(0, t)e^{-i\omega t}\, dt. \tag{16}$$

Equations (14) and (16) represent the complete solution of the time-dependent multimode waveguide problem. In its complete form this formal solution is of little practical value. Thus we proceed to the perturbation solution of a particular problem.

Equation (13) was written in such a way as to suggest a perturbation problem. We added and subtracted the average group velocity v_o in order to obtain the small quantity

$$V = \frac{1}{v_\nu} - \frac{1}{v_o}. \tag{17}$$

V is small since the group velocities of the N modes are only slightly different from each other. Provided we need not include very large values of ω in the analysis ωV can be regarded as a perturbation term in (13). In the spirit of second-order perturbation theory we write the eigenvalue as follows:*

* To first order of perturbation theory only a change in the average group velocity appears. The change of the pulse width depends on the second-order term in (18).

$$\alpha^{(j)}(\omega) = \alpha_0^{(j)} + i\frac{\omega}{v_o} + i\omega\alpha_1^{(j)} + \omega^2\alpha_2^{(j)}. \tag{18}$$

The first term, $\alpha_0^{(j)}$, is the zero-order approximation that corresponds to the solution of the time-independent stationary problem for $\omega = 0$. The terms α_1 and α_2 are first- and second-order perturbation terms. Since the eigenvalue appears in the exponent of an exponential function multiplied by the large quantity z, the perturbation terms can influence the solution (14) very much. The eigenvector $B_\nu(\omega)$ must also be expanded in a similar fashion. However, the zero-order term, $B_{\nu o}$, is by far the most important term in the perturbation series of the eigenvector. The first- and second-order terms of $B_\nu(\omega)$ are of the same relative importance for all values of z and t and can never change very much the zero-order approximation consisting of $B_{\nu o}$ alone. It is therefore sufficient if we approximate $B_\nu(\omega)$ by $B_{\nu o}$. The second-order approximation α_2 is obtained by the well known methods of perturbation theory.

$$\alpha_2^{(i)} = \sum_{\substack{j=1 \\ j\neq i}}^{N} \frac{\left[\sum_{\nu=1}^{N}\left(\frac{1}{v_\nu} - \frac{1}{v_o}\right)B_{\nu o}^{(i)}B_{\nu o}^{(j)}\right]^2}{\alpha_0^{(j)} - \alpha_0^{(i)}}. \tag{19}$$

The range of applicability of the second-order perturbation theory is discussed in the Appendix.

We assume that the input power at $z = 0$ is given by

$$P_\nu(0, t) = G_\nu \exp\left[-(t/\tau)^2\right]. \tag{20}$$

From (16) we obtain

$$c_i(\omega) = \frac{\tau}{2\sqrt{\pi}} k_i \exp\left[-\left(\frac{\tau}{2}\omega\right)^2\right] \tag{21}$$

with

$$k_i = \sum_{\nu=1}^{N} G_\nu B_{\nu o}^{(i)}. \tag{22}$$

The integral appearing in (14) is now of the form

$$I = \int_{-\infty}^{\infty} \exp\left[i\omega\left(t - \frac{z}{v_o} - \alpha_1^{(i)}z\right)\right] \exp\left[-\omega^2\left(\frac{\tau^2}{4} + \alpha_2^{(i)}z\right)\right] d\omega$$

$$= \frac{2\sqrt{\pi}}{(\tau^2 + 4\alpha_2^{(i)}z)^{\frac{1}{2}}} \exp\left\{-\frac{\left[t - \left(\frac{1}{v_o} + \alpha_1^{(i)}\right)z\right]^2}{\tau^2 + 4\alpha_2^{(i)}z}\right\}. \tag{23}$$

The second-order perturbation solution of the multimode waveguide problem with a Gaussian input pulse is thus

$$P_\nu(z, t) = \sum_{i=1}^{N} \frac{\tau}{(\tau^2 + 4\alpha_2^{(i)} z)^{\frac{1}{2}}} k_i B_\nu^{(i)} \cdot \exp(-\alpha_0^{(i)} z) \exp\left\{ -\frac{\left[t - \left(\frac{1}{v_o} + \alpha_1^{(i)} \right) z \right]^2}{\tau^2 + 4\alpha_2^{(i)} z} \right\}. \quad (24)$$

IV. DISCUSSION OF THE RESULT OF PERTURBATION THEORY

Equation (24) contains a description of the propagation of a Gaussian input pulse in a multimode waveguide in case of coupling between the guided modes including radiation losses. However, the solution (24) holds also in the absence of coupling. If we assume, for a moment, that there is no coupling between the guided modes, $h_{\nu\mu} = 0$, and that the only losses are heat losses, $\alpha_\nu = \alpha_h$, we immediately have the following solution of (13):

$$\alpha_0^{(i)} = \alpha_h \quad (25)$$

$$\alpha_1^{(i)} = \frac{1}{v_\nu} - \frac{1}{v_o} \quad (26)$$

$$\alpha_2^{(i)} = 0 \quad (27)$$

$$B_{\nu o}^{(i)} = \delta_{i\nu}. \quad (28)$$

This solution means that the modes are uncoupled, each traveling independently of the others with its own group velocity and with the common attenuation constant α_h. Equation (24) can be written in the absence of coupling

$$P_\nu(z, t) = G_\nu e^{-\alpha_h z} \exp\left\{ -\frac{\left(t - \frac{z}{v_\nu} \right)^2}{\tau^2} \right\}. \quad (29)$$

The input pulse, if spread out over all the modes, arrives at the detector at $z = L$ as a succession of pulses. The total spread in the arrival time of the different pulses is

$$T = \left(\frac{1}{v_N} - \frac{1}{v_1} \right) L. \quad (30)$$

Next, we consider the case that all the modes are coupled among each other, $h_{\nu\mu} \neq 0$. Now the eigenvalues can no longer be written down

explicitly. However, we know from earlier work[7] that there are N eigenvalues with their associated eigenvectors. The eigenvalues can be ordered in sequence such that the zero-order solution $\alpha_0^{(1)}$ has the smallest value while all other zero-order eigenvalues assume increasingly larger values. The lowest-order eigenvalue $\alpha_0^{(1)}$ assumes the meaning of the steady-state loss of the multimode waveguide.[7] The steady-state distribution of power over all the modes is proportional to $B_{\nu o}^{(1)}$. By definition, the steady-state distribution is obtained when the sum in (24) can be approximated by its first term since the exponents $\alpha_0^{(i)}z$ have grown so large that all but the first term in the sum are negligible. In this limit, which always exists provided that the waveguide is long enough, we obtain from (24)

$$P_\nu(z, t) = \frac{\tau}{(\tau^2 + 4\alpha_2^{(1)}z)^{\frac{1}{2}}} k_1 B_{\nu o}^{(1)} \cdot \exp(-\alpha_0^{(1)}z) \exp\left\{-\frac{\left[t - \left(\frac{1}{v_o} + \alpha_1^{(1)}\right)z\right]^2}{\tau^2 + 4\alpha_2^{(1)}z}\right\}. \quad (31)$$

The expression (31) is very different from the expression (29) for the uncoupled modes. Whereas each mode traveled independently of all the others with its own group velocity in the absence of coupling, we see from (31) that all the modes travel with the group velocity

$$v_o = \frac{1}{\frac{1}{v_o} + \alpha_1^{(1)}} \quad (32)$$

once the steady-state distribution is established. The term $\alpha_1^{(1)}$ can always be made to vanish by suitable choice of v_o. Furthermore we see that, to the approximation implicit in (31), the pulse remains Gaussian. All the modes suffer identical attenuation according to the attenuation constant $\alpha_0^{(1)}$. The distribution of power over all the modes is determined by the lowest-order eigenvector $B_{\nu o}^{(1)}$. The other eigenvectors have no physical meaning. In fact, these higher eigenvectors can have negative elements whereas the power in each mode must be a positive quantity. Most important for our present discussion is the width of the Gaussian pulse. We see that at $z = L$ it is given by the expression

$$\Delta t = 2(\tau^2 + 4\alpha_2^{(1)}L)^{\frac{1}{2}}. \quad (33)$$

The pulse width increases as the multimode package travels along

the waveguide. For sufficiently large values of L we have $\tau \ll 4\alpha_2^{(1)}L$ and the pulse width becomes proportional to the square root of L. We can define an improvement factor R by the relation

$$R = \frac{\Delta t}{T} = \frac{2(\tau^2 + 4\alpha_2^{(1)}L)^{\frac{1}{2}}}{\left(\frac{1}{v_N} - \frac{1}{v_1}\right)L}. \tag{34}$$

If the width of the input pulse is much less than $4\alpha_2^{(1)}L$, (34) simplifies:

$$R = \frac{4\sqrt{\alpha_2^{(1)}}}{\left(\frac{1}{v_N} - \frac{1}{v_1}\right)\sqrt{L}}. \tag{35}$$

It is apparent that for sufficiently large values of L the improvement factor R, describing the shortening of the pulse as a result of mode coupling, is less than unity.

It is possible to express the loss suffered by the pulse directly as a function of the improvement factor R. The power loss of the multimode signal is given by $\alpha_0^{(1)}L$. If we are interested only in the loss penalty that must be paid for a certain improvement R we can express L in terms of R with the help of (35) and obtain for the loss per improvement R

$$\alpha_0^{(1)}L_R = 16\,\frac{\alpha_0^{(1)}\alpha_2^{(1)}}{\left(\frac{1}{v_N} - \frac{1}{v_1}\right)^2 R^2}. \tag{36}$$

The actual length of waveguide required to incur the loss (36) does no longer appear on the right-hand side. The loss penalty is thus expressed in terms of the zero-order eigenvalue $\alpha_0^{(1)}$ and its second-order perturbation $\alpha_2^{(1)}$, the difference in the group velocities of the first and Nth mode and the desired improvement R. Methods of minimizing this loss penalty occupy most of the remainder of this paper. The length required to obtain a certain pulse width or a certain improvement in the spreading of the pulse is determined by the second-order perturbation $\alpha_2^{(1)}$ of the eigenvalue of the lowest-order mode.

V. APPLICATION TO SLAB WAVEGUIDES

The coupling coefficients $h_{\nu\mu}$ were obtained in Ref. 7 for the case of a slab waveguide. The coupling mechanism is assumed to be the irregular boundary between the core and the cladding of the waveguide. The cladding is assumed to be infinitely extended. In Ref. 7 we assumed

that the function describing the core-cladding interface irregularity had a Gaussian correlation function. Dropping this restriction and expressing the coupling coefficient in terms of the "power spectrum" $F(\beta_\nu - \beta_\mu)$ of the core-cladding interface function $f(z)$ we obtain for the slab waveguide[7]

$$h_{\nu\mu} = \frac{n_1^2 k^2 \sin^2 \theta_\nu \sin^2 \theta_\mu}{2d^2\left(1 + \frac{1}{\gamma_\nu d}\right)\left(1 + \frac{1}{\gamma_\mu d}\right) \cos \theta_\nu \cos \theta_\mu} F(\beta_\nu - \beta_\mu). \tag{37}$$

The parameters appearing in this equation have the following meaning:

n_1 = refractive index of core material
n_2 = refractive index of cladding material
$k = 2\pi/\lambda$ = free-space propagation constant
d = half-width of core
β_ν = propagation constant of mode ν
θ_ν = characteristic angle of mode ν

$$\gamma_\nu = (\beta_\nu^2 - n_2^2 k^2)^{\frac{1}{2}} \tag{38}$$

$$\cos \theta_\nu = \frac{\beta_\nu}{n_1 k}. \tag{39}$$

Values for the radiation losses α_ν were given in Ref. 7. In this paper we consider only relatively narrow "power spectra" $F(\phi)$ coupling each mode only to its nearest neighbor or at the most to a few of its neighbors. In this case only the highest-order mode is coupled to the radiation field. It has been determined by trying out different numerical examples that the radiation losses of the coupled mode system do not depend critically on the loss value α_N, provided that it is large enough. We thus use

$$\left.\begin{aligned} \alpha_\nu &= 0 \qquad \nu \neq N \\ \alpha_N &\to \infty \end{aligned}\right\}. \tag{40}$$

The reason for this insensitivity of the multimode losses on the value of α_N can be explained if we consider that power coupled from any of the guided modes to mode N is quickly lost to radiation. The actual rate of loss from mode N to the radiation modes is not important as long as this rate is high. The actual losses of the multimode guide are determined by the rate at which power flows from mode $N - 1$ to mode N. This rate is determined correctly by the coupling coefficient $h_{N,N-1}$. It is thus not necessary to know the exact values of α_ν. For

actual computations (40) was used with values for α_N that were several orders of magnitude larger than $\alpha_0^{(1)}$.

In Ref. 7 we described the propagation constant of the guided slab modes by using the approximation that is valid far from cutoff. This approximation is based on using

$$\kappa_\nu d = \nu \frac{\pi}{2} \tag{41}$$

with

$$\kappa_\nu = n_1 k \sin \theta_\nu \tag{42}$$

or

$$\beta_\nu = (n_1^2 k^2 - \kappa_\nu^2)^{1/2}. \tag{43}$$

The mode number ν assumes all values from 1 through N with odd numbers indicating even modes while even numbers indicate odd modes. For our present purpose this approximation is not accurate enough since we are interested in accurate values for $\alpha_0^{(1)}$ and $\alpha_2^{(1)}$, particularly in the region where the guided modes are coupled only by the tail of the "power spectrum," so that the spacing between the modes has a critical influence on the actual values of the parameters. Therefore, we chose to use the exact values for κ_ν, β_ν, and γ_ν which are obtained as solutions of the eigenvalue equation

$$\tan \kappa_\nu d = \frac{\gamma_\nu}{\kappa_\nu} \tag{44}$$

for even guided TE modes and from

$$\tan \kappa_\nu d = -\frac{\kappa_\nu}{\gamma_\nu} \tag{45}$$

for odd TE modes. We restrict ourselves to those modes of the slab waveguide that have no variation in y direction and can thus be classified as TE and TM modes. However, only TE modes are being considered. The solutions of (44) and (45) with $n_1 = 1.5$ and $n_1/n_2 = 1.01$ are given in Table I for three particular cases of 5-, 10-, 20-, and 39-mode operation. Also shown in this table are the differences between adjacent values of β_ν. These numbers make it apparent how the spacing between the guided modes increases with increasing mode number. It is also interesting to compare the values of Table I with the approximation (41). It is apparent that (41) approximates the actual values better for the modes of low order in waveguides that support many modes.

TABLE I—PARAMETERS FOR THE TE MODES OF THE SLAB WAVEGUIDE FOR $n_1/n_2 = 1.01$

ν	$\kappa_\nu d$	$\beta_\nu d$	$(\beta_\nu - \beta_{\nu+1})d$
$kd = 35$, 5-mode case ($n_1 = 1.5$, $n_1/n_2 = 1.01$)			
1	1.3821	52.48180	0.05429
2	2.7580	52.42751	0.08936
3	4.1193	52.33815	0.12187
4	5.4507	52.21628	0.14679
5	6.7096	52.06949	———
$kd = 70$, 10-mode case			
1	1.4708	104.98970	0.03089
2	2.9407	104.95881	0.05140
3	4.4086	104.90741	0.07281
4	5.8733	104.83560	0.09199
5	7.3332	104.74361	0.11186
6	8.7861	104.63175	0.13115
7	10.2286	104.50060	0.14939
8	11.6544	104.35121	0.16531
9	13.0498	104.18590	0.17295
10	14.3634	104.01295	———
$kd = 145$, 20-mode case			
1	1.5210	217.49468	0.01595
2	3.0418	217.47873	0.02658
3	4.5624	217.45214	0.03721
4	6.0826	217.41493	0.04783
5	7.6023	217.36710	0.05844
6	9.1214	217.30865	0.06904
7	10.6396	271.23961	0.07962
8	12.1568	217.15999	0.09018
9	13.6728	217.06981	0.10070
10	15.1873	216.96911	0.11119
11	16.7000	216.85793	0.12161
12	18.2105	216.73631	0.13197
13	19.7182	216.60434	0.14222
14	21.2226	216.46213	0.15231
15	22.7225	216.30981	0.16218
16	24.2167	216.14764	0.17168
17	25.7028	215.97596	0.18051
18	27.1767	215.79545	0.18789
19	28.6291	215.60757	0.19023
20	30.0270	215.41733	———

VI. THE DEPENDENCE OF THE LOSS PENALTY ON THE SHAPE OF THE "POWER SPECTRUM"

We observed earlier that a "power spectrum" of the core-cladding interface function of the form shown in Fig. 2 would couple all the guided modes (except mode N) without causing radiation losses. Unfortunately, it is not possible to design dielectric waveguides with core-cladding interfaces whose power spectrum cuts off abruptly at a given specified mechanical frequency. It is thus necessary to study the loss penalty (36) for different "power spectra" in order to determine its dependence on the slope of the "power spectrum."

TABLE I—PARAMETERS FOR THE TE MODES OF THE SLAB WAVEGUIDE FOR $n_1/n_2 = 1.01$ (Continued)

ν	$\kappa_\nu d$	$\beta_\nu d$	$(\beta_\nu - \beta_{\nu+1})d$
$kd = 290$, 39-mode case			
1	1.5455	434.99725	0.00824
2	3.0909	434.98901	0.01373
3	4.6364	434.97529	0.01922
4	6.1818	434.95607	0.02471
5	7.7271	434.93136	0.03020
6	9.2723	434.90117	0.03569
7	10.8175	434.86547	0.04118
8	12.3625	434.82430	0.04667
9	13.9074	434.77762	0.05216
10	15.4521	434.72546	0.05765
11	16.9967	434.66782	0.06314
12	18.5410	434.60468	0.06862
13	20.0852	434.53605	0.07411
14	21.6291	434.46194	0.07960
15	23.1727	434.38235	0.08508
16	24.6160	434.29727	0.09056
17	26.2590	434.20671	0.09605
18	27.8016	434.11066	0.10152
19	29.3438	434.00914	0.10699
20	30.8856	433.90215	0.11246
21	32.4269	433.78969	0.11792
22	33.9676	433.67176	0.12339
23	35.5077	433.54838	0.12883
24	37.0472	433.41955	0.13428
25	38.5859	433.28572	0.13970
26	40.1237	433.14557	0.14512
27	41.6606	433.00045	0.15052
28	43.1964	432.84993	0.15589
29	44.7310	432.69404	0.16124
30	46.2642	432.53280	0.16655
31	47.7956	432.36625	0.17181
32	49.3251	432.19444	0.17701
33	50.8521	432.01743	0.18212
34	52.3762	431.83531	0.18710
35	53.8964	431.64821	0.19188
36	55.4114	431.45633	0.19630
37	56.9191	431.26003	0.20007
38	58.4149	431.05996	0.20201
39	59.8867	430.85796	

We begin by considering a "power spectrum" that couples all the guided modes equally except for the last two modes that are coupled by the tail of the "power spectrum" distribution. By equally coupled modes we mean that the "power spectrum" remains flat in the region that contributes to coupling between the guided modes. The actual amount of coupling depends, in addition to the "power spectrum," on the mode angles θ_ν [see equation (37)] so that a constant power spectrum couples higher-order modes more strongly than lower-order modes.

The "power spectrum" that is used as a model for a more realistic case is shown in Fig. 3. The flat portion of this spectrum couples mode $N-1$ to mode $N-2$, mode $N-2$ to mode $N-3$, etc., finally coupling several of the low-order modes among each other. Mode N is coupled to mode $N-1$ via the tail of the power spectrum distribution. The factor of importance in this discussion is the level to which the "power spectrum" has decayed from its maximum value at the point that is instrumental in coupling the last two modes to each other. Strong coupling of the last two modes leads to high radiation losses since it causes more power to flow from the guided modes to the radiation modes. The last mode, mode N, couples strongly to the radiation modes since the flat part of the spectrum connects this mode with the continuum of radiation modes. As explained earlier, we do not bother to compute the exact value of the coupling coefficient of mode N to the radiation field since it depends critically on the exact shape of the tail of the "power spectrum," complicating the discussion. Furthermore, it has been established that the actual amount of coupling of mode N to the radiation modes has no influence on the radiation losses of the multimode waveguide as long as the coupling exceeds a certain threshold value. At worst we may overestimate the radiation losses by assigning a large but arbitrary value to the parameter α_N.

Using the "power spectrum" of Fig. 3, we determine the loss penalty of equation (36). Analytically, we express the power spectrum as follows:

$$F(\phi) = \begin{cases} \dfrac{\pi\sigma^2}{\beta_{N-2} - \beta_{N-1}} & \text{for } |\phi| \leqq \beta_{N-2} - \beta_{N-1} \\ K\dfrac{\pi\sigma^2}{\beta_{N-2} - \beta_{N-1}} & \text{for } |\phi| = \beta_{N-1} - \beta_N \end{cases} . \tag{46}$$

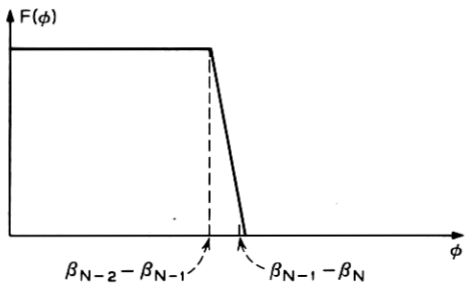

Fig. 3—A more realistic model of the desirable core-cladding interface "power spectrum."

The factor K determines the fraction of the maximum value to which the "power spectrum" has decayed at the point $\phi = \beta_{N-1} - \beta_N$ that is instrumental in coupling mode $N - 1$ to mode N.

The actual calculation is based on the slab waveguide model. According to (13) we must solve the zero-order eigenvalue problem

$$HB^{(i)} = -\alpha_0^{(i)} B^{(i)}. \tag{47}$$

$B^{(i)}$ is a column vector whose elements are $B_{\nu o}^{(i)}$ and H is a matrix with the elements

$$H_{\nu\mu} = h_{\nu\mu} - (\alpha_\mu + b_\mu)\delta_{\nu\mu} \tag{48}$$

that are determined by (8), (37), and (40). The eigenvalues $\alpha_0^{(i)}$ and eigenvectors $B_{\nu o}^{(i)}$ are determined numerically with the help of a computer. Using the result of the zero-order calculation we calculate $\alpha_2^{(1)}$ from equation (19). Instead of $\alpha_0^{(1)}$ and $\alpha_2^{(1)}$, the normalized dimensionless quantity

$$\bar{\alpha}_0^{(1)} = \frac{d}{\sigma^2 k^2} \alpha_0^{(1)} \tag{49}$$

was used in Ref. 7. In this paper the second-order perturbation of the eigenvalues is plotted in the following normalized form:

$$\bar{\alpha}_2^{(1)} = v_o^2 \frac{\sigma^2 k^2}{d} \alpha_2^{(1)}. \tag{50}$$

These normalizations have the advantage of removing the rms deviation σ of the core-cladding interface from the equations so that we need not specify any particular value for this parameter. Figure 4 shows a plot of the normalized* loss penalty $R^2\alpha_0^{(1)}L_R$ as a function of the factor K defined by the second line of (46). The four curves appearing in Fig. 4 were calculated for $kd = 35$ resulting in 5 guided modes, $kd = 70$ corresponding to 10 guided modes, $kd = 145$ or the 20-mode case, and finally for $kd = 290$ which gives 39 guided modes. The curve for 39 modes seems to deviate from the straight line beyond the region for which it appears drawn out in Fig. 4. Since the numerical diagonalization of a 39 by 39 element matrix is quite expensive no attempt was made to explore the precise shape of this curve.

Let us study the 10-mode case in more detail. For $K = 10^{-4}$ we find from Fig. 4 the value $R^2\alpha_0^{(1)}L_R = 0.01$ dB. This means that if we want to obtain a reduction of the uncoupled pulse distortion by a factor of

* This normalization involves only the factor R^2 and is unrelated to (49).

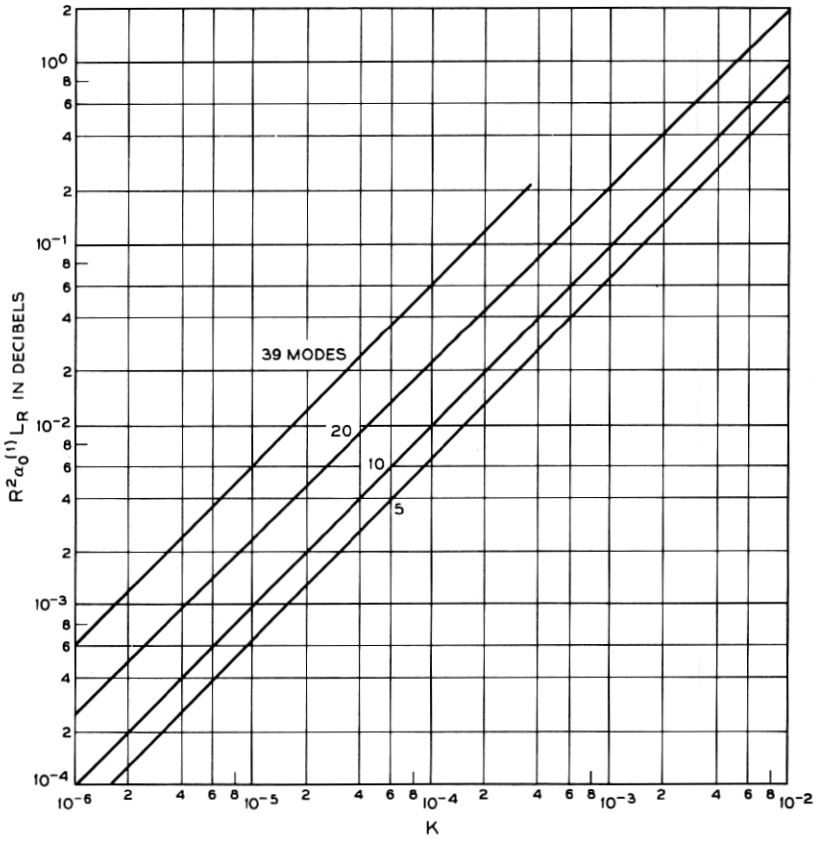

Fig. 4—The loss penalty $R^2\alpha_0{}^{(1)}L_R$ (in dB) that must be paid for a pulse distortion reduction R, ($R < 1$). The variable K is the fraction to which the "power spectrum" has decayed from its flat region at the point where it couples mode $N - 1$ to mode N.

$R = 0.1$, we would have to pay a loss penalty of 1 dB. A reduction of $R = 0.033$ would have to be paid for with 10 dB radiation loss. Let us next consider the slope of the "power spectrum". For the 10-mode case we have according to Table I $(\beta_8 - \beta_9)d = 0.165$. The width of the flat portion of Fig. 3 is thus $0.165/d$. Since $(\beta_9 - \beta_{10})d = 0.173$ we must require that the spectrum drop from unity to 10^{-4} in the "distance" $0.008/d$. The ratio of the region of the slope to the width of the flat region is thus $0.008/0.165 = 0.05$ or the slope extends over 5 percent of the flat portion of the spectrum. For the 39-mode case we obtain correspondingly $(\beta_{37} - \beta_{38})d = 0.2$ and $(\beta_{38} - \beta_{39})d = 0.202$;

the ratio of slope width to the width of the flat part of the spectrum is thus 0.002/0.2 = 0.01 or 1 percent. This comparison shows that the relative width of the slope region must be smaller if more modes can propagate on the waveguide. The "power spectrum" considered for these two examples results in a steady-state power distribution that puts nearly equal power into all the modes with the exception of the last mode which carries essentially no power because of its strong coupling with the radiation modes.

The pulse distortion expected for these examples can be obtained from the data in Table II. In the absence of mode coupling the pulse distortion is given by (30). The inverse of the group velocity of the slab waveguide modes can be calculated with the help of the eigenvalue equations (44) and (45),

$$\frac{1}{v_\nu} = \frac{\partial \beta_\nu}{\partial \omega} = \frac{\beta_\nu^2 + n_1^2 k^2 \gamma_\nu d}{\omega \beta_\nu (1 + \gamma_\nu d)}. \tag{51}$$

The center column of Table II provides the values of T/L. The last column contains the normalized second-order perturbation of the eigenvalues of the matrix eigenvalue problem (13) which is almost independent of K. Given a desired improvement factor, we can calculate the required length L for given rms deviation σ of the core-cladding interface or, vice versa, obtain the rms deviation σ from the given guide length L. Let us consider the following example. We assume that the waveguide length is given as $L = 1$ km, the wavelength of the light signal is $\lambda = 1$ μm. The numerical values in our figures and tables apply to the case $n_1 = 1.5$ and $n_1/n_2 = 1.01$. We want to obtain a pulse distortion improvement resulting in $R = 0.1$. Table III shows

TABLE II—NUMERICAL VALUES FOR THE PULSE DISTORTION IN THE ABSENCE OF COUPLING (THIRD COLUMN) AND THE NORMALIZED SECOND-ORDER PERTURBATION OF THE EIGENVALUE (FOURTH COLUMN) IN THE PRESENCE OF COUPLING FOR THE "POWER SPECTRUM" OF EQUATION (46)

(The normalized second-order perturbation is nearly independent of K)

Number of Modes	kd	$\frac{c}{n_1}\left(\frac{1}{v_N} - \frac{1}{v_2}\right) = \frac{cT}{n_1 L}$	$v_o^2 \frac{\sigma^2 k^2}{d} \alpha_2^{(1)}$
5	35	3.94×10^{-3}	0.02
10	70	5.02×10^{-3}	0.07
20	145	6.69×10^{-3}	0.4
39	290	8.13×10^{-3}	2.0

TABLE III—NUMERICAL VALUES FOR THE EXAMPLE LISTED IN TABLE II CORRESPONDING TO THE "POWER SPECTRUM" OF EQUATION (46) OR FIG. 3

($R = 0.1$, $\lambda = 1$ μm, $K = 10^{-4}$, $L_R = 1$ km)

Number of Modes	d(μm)	T(s)	σ(μm)	$\alpha_o{}^{(1)}L_R$(dB)
5	5.57	1.97×10^{-8}	1.71×10^{-2}	0.63
10	11.1	2.51×10^{-8}	3.56×10^{-2}	1
20	23.1	3.35×10^{-8}	9.16×10^{-2}	2.3
39	46.2	4.07×10^{-8}	2.39×10^{-1}	6

the numerical values of several interesting quantities that follow for this example from Fig. 4 and Table II with the ordinate value of Fig. 3, $K = 10^{-4}$. Listed in Table III are the slab half-width d, the time T to which an infinitely narrow input pulse is stretched out in the absence of coupling (pulse distortion caused by frequency dispersion in the material and due to waveguide effects is not being considered), the rms core-cladding interface irregularity that is required to provide the proper amount of coupling to achieve a pulse distortion improvement of $R = 0.1$ over a distance of $L = 1$ km, and finally, in the last column of the table, the loss penalty that results from $R = 0.1$. The most remarkable result of this example is the fact that such a slight core-cladding interface irregularity is so effective in coupling the guided modes. There may be problems in designing an optical fiber with such a slight core-cladding irregularity. In particular it might be expected that random core-cladding interface irregularities exist whose spectrum is very different from the desired shape shown in Fig. 3. Such unwanted core-cladding interface irregularities would be detrimental since they provide unwanted radiation losses. If the desired core-cladding interface irregularity is made larger, the multimode pulse dispersion is improved more than the factor $R = 0.1$ assumed here. However, such an improved mode mixing must be paid for with a higher loss penalty that can be reduced only by decreasing the factor K [the ordinate in Fig. 4; see also equation (46)].

The "power spectrum" of Fig. 3 is not realizable in practice and was used only to gain insight into the relation between pulse distortion improvement and loss penalty. It is interesting to pursue this question further and study other "power spectra." An obvious choice is a "power spectrum" of the form

$$F(\phi) = \frac{m\sigma^2 \sin \frac{\pi}{m}}{\Delta\beta\left[1 + \left|\frac{\phi}{\Delta\beta}\right|^m\right]}. \tag{52}$$

It can be seen in Fig. 5 that (52) approximates the idealized power spectrum of Fig. 3 for large values of m. The "power spectrum" (52) has the advantage of making it possible to study the loss penalty not only as a function of the slope of the power spectrum but also as a function of its width $\Delta\beta$. Figure 6 shows a number of loss penalty curves for the 10-mode case as a function of the width parameter $\Delta\beta d$ of the "power spectrum" (52). The curve parameter is the exponent m. Figure 6 reveals several interesting properties of the loss penalty in relation to the shape of the "power spectrum". The curves shown in Fig. 6 have a maximum. To the right of this maximum the loss penalty is decreasing very rapidly making it appear as though this were a good region of operation. However, a more detailed investigation of the lowest-order eigenvector $B_{\nu_0}^{(1)}$ reveals that the steady-state power distribution in the region to the right of the maximum in Fig. 6 permits

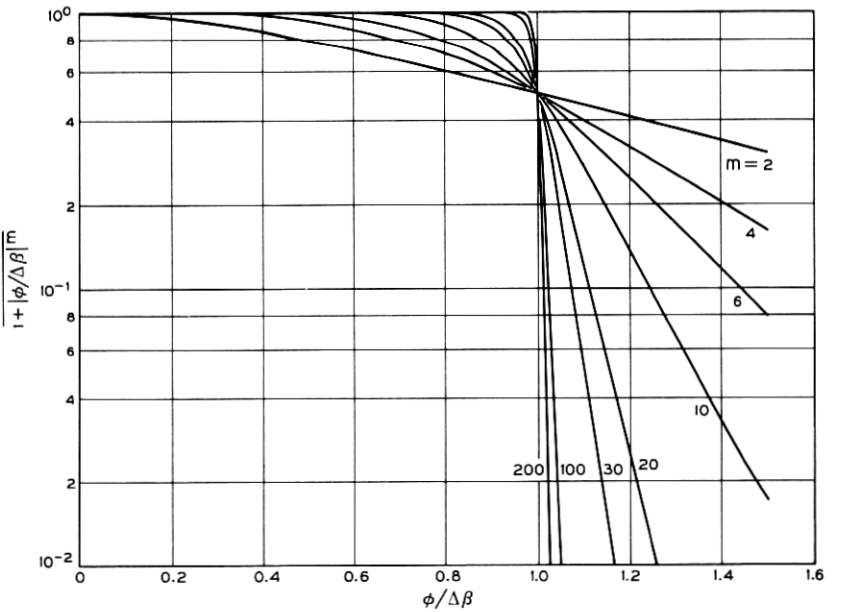

Fig. 5—A simple power law model for the "power spectrum."

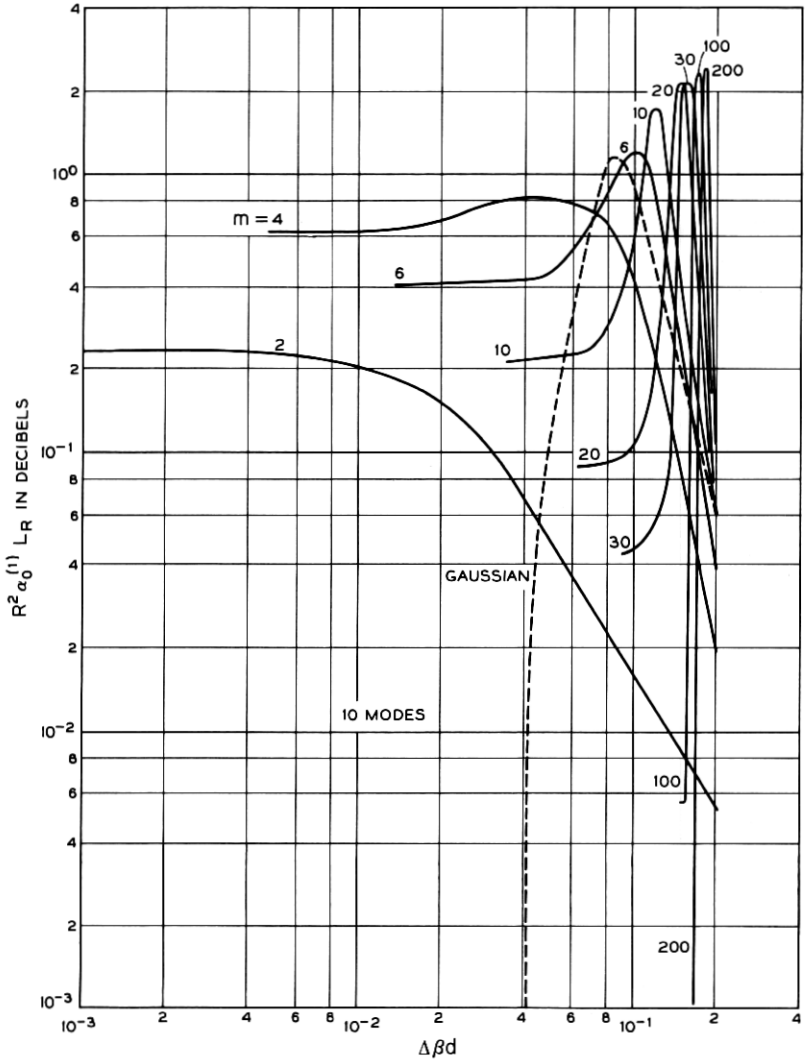

Fig. 6—The loss penalty for the "power spectrum" of Fig. 5 for $n_1/n_2 = 1.01$.

power to remain essentially only in the lower-order modes. This mode of operation is, of course, favorable from the point of view of pulse distortion. But if the fiber is to be excited with a light-emitting diode feeding power equally into all the modes, most of the power is lost in the transient before the steady-state power distribution establishes

itself. The region to the right of the maxima is thus considered to be unsuitable for efficient power transmission in a multimode waveguide. To the left of the maxima we find a sharp drop off ending in a plateau. On the left slope of the curve we enter a region in which all the modes of the waveguide share more evenly the total amount of power carried by the guide. On the plateaus the power distribution versus mode number is flat. The plateau regions are thus desirable from the point of view of efficient multimode operation with reduced pulse dispersion. Unfortunately the level of the loss penalty is rather high for low values of the exponent. We see also that the plateau regions move to the left for decreasing values of the exponent m. This indicates that low loss can be achieved only if the high-order modes are coupled only through the tails of the "power spectrum" curve. The last column of Table I gives for $\nu = 8$ the value of $(\beta_8 - \beta_9)d = 0.165$ for the 10-mode case. Since $(\beta_9 - \beta_{10})d = 0.173$, this means that the ideal region of operation would be $0.173 > \Delta\beta d > 0.165$ and $m \to \infty$. Figure 6 shows clearly the trend in this direction. For lower values of m the point of operation must be shifted to much smaller values of $\Delta\beta d$ and is accompanied by an increase in the loss penalty in the plateau region. Simultaneously with decreasing loss we obtain a decrease in the coupling between the guided modes. This behavior is very apparent in Fig. 7 which shows a plot of the normalized second-order perturbation of the eigenvalue which, as we know, determines the width of the steady state Gaussian pulse. In the plateau regions of Fig. 6 the normalized value of $\alpha_2^{(1)}$ becomes very large indicating a rapidly decreasing efficiency of pulse delay distortion reduction. The actual value of the length of the Gaussian pulse or of the improvement factor R is, of course, dependent on the rms deviation σ of the core-cladding interface. The flattening out of the loss penalty curves in the plateau region can be attributed to the fact that the loss of coupling efficiency among the guided modes with decreasing width of the "power spectrum" is accompanied by a corresponding reduction in power transfer to the radiation modes.

The region immediately to the left of the plateaus shown in Fig. 6 is interesting also. We terminated the curves since the numerical matrix diagonalization routine failed to function for values of $\Delta\beta d$ to the left of the end of each curve. This mathematical phenomenon has an important physical reason. As the coupling between the guided modes decreases, we encounter a regime of instability where the steady-state power distribution depends on the initial power distribution. In the absence of coupling each arbitrary power distribution is a steady-state distribution since power is no longer exchanged between the

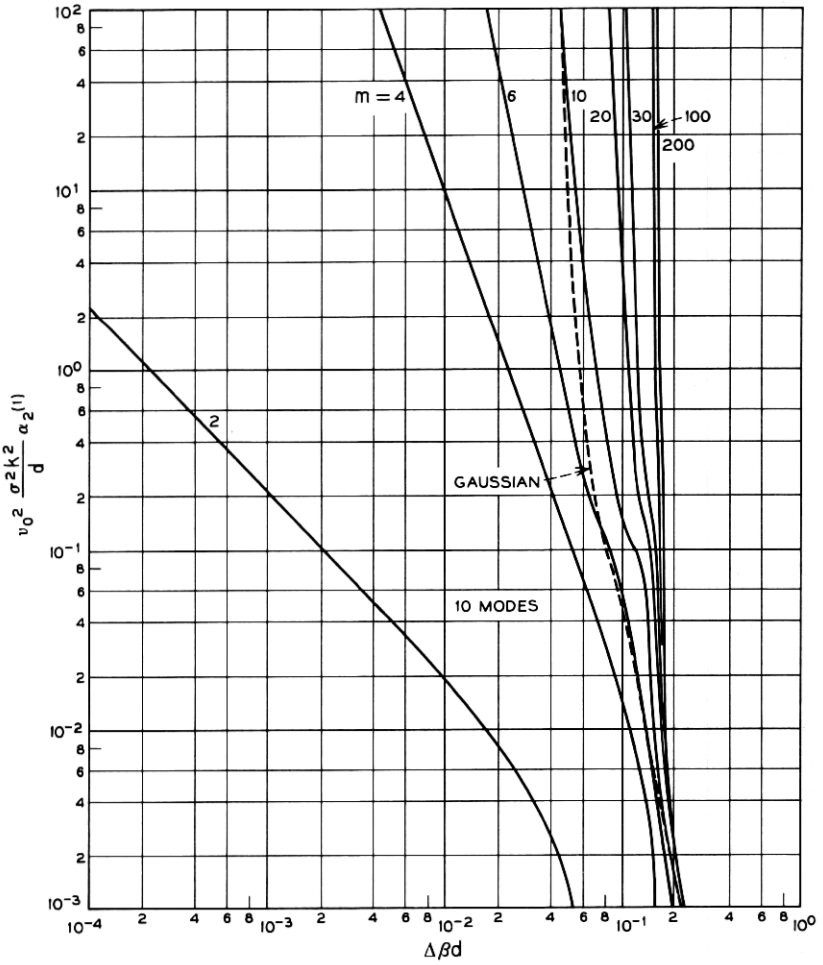

Fig. 7—The normalized second-order perturbation of the eigenvalue (this parameter determines the width of the pulse) $\alpha^{(1)}$ as a function of the width parameter of the "power spectrum" of Fig. 5. $n_1/n_2 = 1.01$.

modes. The onset of this instability causes the matrix diagonalization routine to fail. In fact, it is interesting to observe how different matrix diagonalization programs return different eigenvectors and eigenvalues in the region to the left of the plateaus. This phenomenon does not indicate errors in these programs but shows that the final solution depends on random fluctuations and is no longer uniquely determined. It is clear that the regions to the left of the plateaus are unsuitable for

purposes of pulse distortion reduction by means of mode coupling. Figure 6 thus shows that significant pulse distortion reduction with low loss penalty is possible at least in principle by using a very large value of the exponent m and operating at the lowest point of the steep slopes to the left of the maxima. The required tolerances for $\Delta\beta d$ become increasingly more critical as the value of the exponent m is being increased.

The curve for $m = 2$ in Fig. 6 remains entirely in the region, corresponding to the right of the maxima of the remaining curves, where most of the power is carried by the lower-order modes. The power spectrum (52) with $m = 2$ is thus unsuitable for our purposes. For comparison purposes Fig. 6 shows the loss penalty for the Gaussian "power spectrum,"

$$F(\phi) = \frac{2\sqrt{\pi}\,\sigma^2}{\Delta\beta} \exp\left[-\left(\frac{\phi}{\Delta\beta}\right)^2\right], \tag{53}$$

as a dotted line.

For large values of m the curves of Fig. 7 are not very suitable for computing the required rms deviation σ for given values of R and L because of their extremely steep slopes. It is advisable to use Fig. 5 and the values for the propagation constant differences of Table I to define an equivalent factor K [compare (46)] and use Fig. 4 for obtaining the loss penalty and Table II for obtaining the value of the normalized second-order perturbation of the lowest-order eigenvalue. (This value is very nearly independent of K. The steep slopes of the curves of Fig. 7 result from their sensitive dependence on $\Delta\beta d$.) Instead, we consider as an example a moderately large value of m. Let us assume that $m = 20$ and let us use $R = 0.1$, $L = 1$ km, $\lambda = 1$ μm, and the 10-mode case, $kd = 70$. Choosing as the operating point $\Delta\beta d = 0.1$ we obtain from Fig. 6 the loss penalty $\alpha_0^{(1)} L_R = 10$ dB. From Fig. 7 we find

$$v_0^2 \frac{\sigma^2 k^2}{d} \alpha_2^{(1)} = 4.2. \tag{54}$$

The difference of the group velocities of mode 1 and mode 10 follows from Table II. We thus obtain, with the help of (35), $\sigma = 0.27$ μm. This example results in ten times higher loss than the 10-mode case listed in Table III but the required rms deviation is more easily realizable than that of Table III.

Figures 6 and 7 apply to the 10-mode case. In order to explore the dependence of the loss penalty and the pulse length factor $\alpha_2^{(1)}$ on the

number of modes, Fig. 8 shows a comparison of the loss penalty for the exponent $m = 10$ [see (52)] for 5, 10, 20, and 39 modes as a function of the "power spectrum" width parameter $\Delta\beta d$. The curve for $N = 39$ was not extended out of the plateau region because of the cost involved in the diagonalization of the large matrix. The curves of Fig. 8 show that the loss penalty decreases slowly with increasing mode number. It appears that the dependence of the loss penalty in the plateau region on the mode number is approximately given by $N^{-1/2}$ for large values of N. The curve for $N = 5$ does not obey this law, possibly because this number is still too small.

The corresponding dependence of the normalized second-order perturbation of the eigenvalue on mode number is shown in Fig. 9. The two points for the curve of $N = 39$ in the region shown in Fig. 8 lie above the range of the figure.

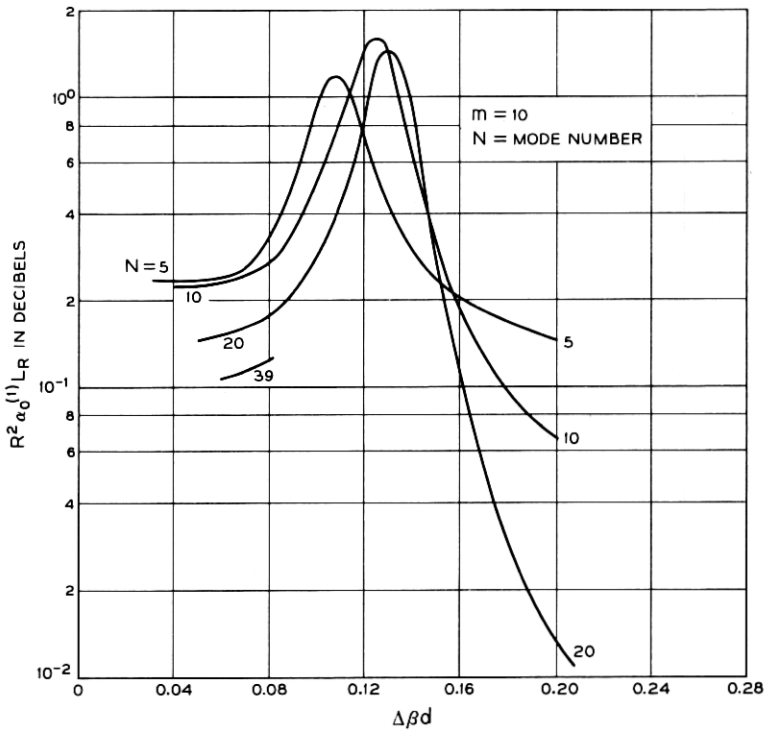

Fig. 8—Mode dependence of the loss penalty for $m = 10$ is shown as a function of the width parameter of the "power spectrum."

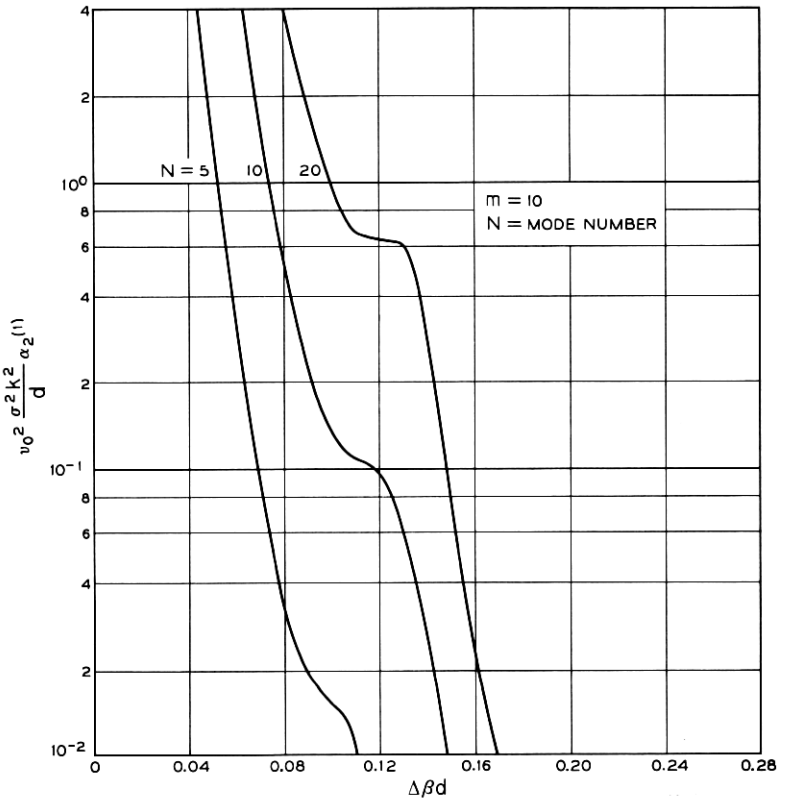

Fig. 9—The second-order perturbation of the eigenvalue $\alpha^{(1)}$ for three different mode numbers as a function of the width parameter of the power spectrum for $m = 10$.

In order to obtain an insight into the meaning of these curves (Figs. 8 and 9), Table IV presents the rms deviation that is required to achieve a pulse distortion improvement of $R = 0.1$ at $\Delta\beta d = 0.08$ for $\lambda = 1$ μm. The required values of the rms deviation are only slightly larger than those listed in Table III but the loss penalty for a pulse distortion reduction of $R = 0.1$ is far higher since the numbers in Table IV pertain to a relatively small value of the exponent, $m = 10$.

VII. DEPENDENCE ON THE REFRACTIVE INDEX DIFFERENCE

So far, all our examples applied to dielectric slab waveguides with a core-to-cladding-index ratio of $n_1/n_2 = 1.01$. In order to explore the

TABLE IV—NUMERICAL VALUES FOR AN EXAMPLE BASED ON THE "POWER SPECTRUM" OF EQUATION (52) OR FIG. 5

($R = 0.1$, $\lambda = 1$ μm, $\Delta\beta d = 0.08$, $m = 10$, $L_R = 1$ km)

Number of Modes	$\sigma(\mu m)$	$\alpha_o^{(1)} L_R$(dB)
5	2.16×10^{-2}	33
10	9.44×10^{-2}	27
20	2.97×10^{-1}	17
39	7.96×10^{-1}	12

dependence of our results on the index differences we give a few data for the case $n_1/n_2 = 1.005$. Table V shows results similar to those of Table I for the 10-mode case. The most important differences of these two examples are the increase of the value of kd required to obtain 10 guided modes from 70 for $n_1/n_2 = 1.01$ to $kd = 97$ for $n_1/n_2 = 1.005$. In addition, we find that the values for $(\beta_\nu - \beta_{\nu+1})d$ have become smaller. The "power spectrum" of the core-cladding interface irregularities must thus become narrower and have steeper slopes in order to yield the same loss penalty in both cases. The task of designing this "power spectrum" is thus more difficult for smaller index differences between core and cladding. The loss penalty that must be paid in this case is shown in Fig. 10 which is similar to Fig. 6 except that the abscissa is now represented on a linear scale. A few of the curves of Fig. 6 are also shown in Fig. 10 as dotted lines for comparison purposes. It is apparent that the smaller index difference causes the curves to shift

TABLE V—PARAMETERS FOR THE TE MODES OF THE SLAB WAVEGUIDE FOR $n_1/n_2 = 1.005$

[$kd = 97$, 10-mode case ($n_1 = 1.5$, $n_1/n_2 = 1.005$)]

ν	$\kappa_\nu d$	$\beta_\nu d$	$(\beta_\nu - \beta_{\nu+1})d$
1	1.4693	145.49258	0.02224
2	2.9375	145.47034	0.03700
3	4.4037	145.43334	0.05166
4	5.8665	145.38168	0.06615
5	7.3243	145.31553	0.08036
6	8.7746	145.23517	0.09410
7	10.2137	145.14107	0.10699
8	11.6347	145.03408	0.11791
9	13.0213	144.91617	0.12071
10	14.3012	144.79546	

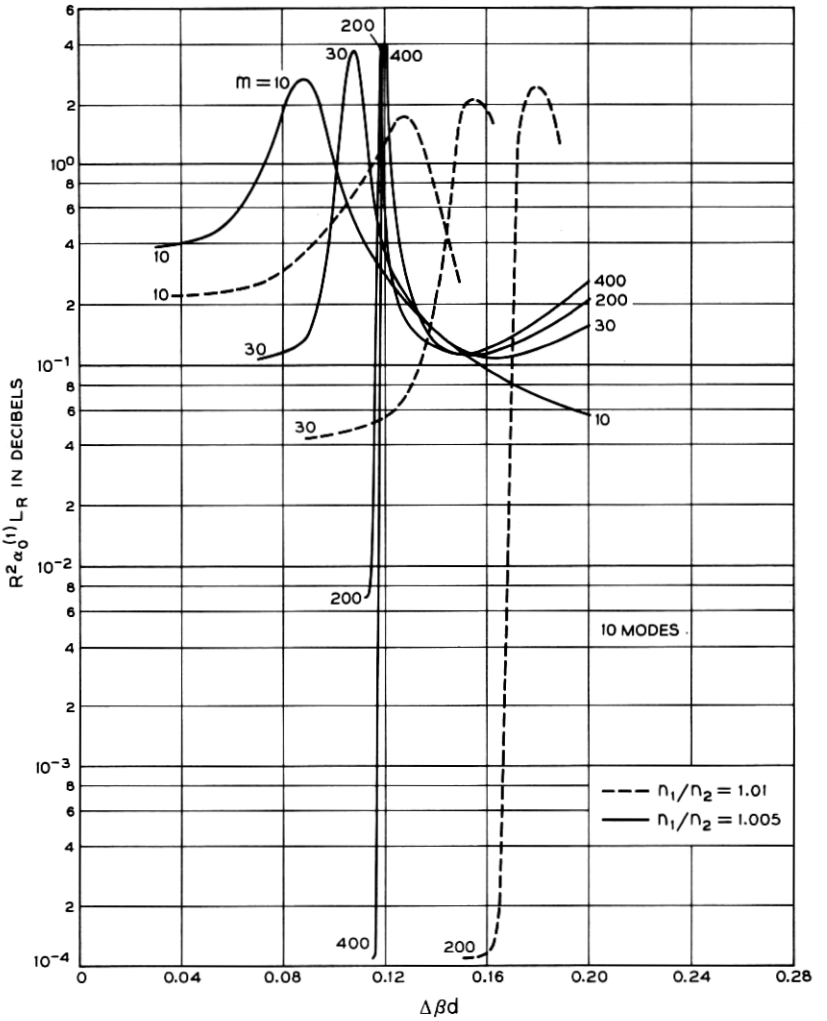

Fig. 10—The loss penalty for the "power spectrum" of Fig. 5. The solid lines apply to the case $n_1/n_2 = 1.005$, the dotted lines are drawn in for comparison with the case $n_1/n_2 = 1.01$.

to the left. Furthermore, we see that the loss penalty is increased for a given value of m.

The normalized second-order perturbation of the lowest-order eigenvalue is shown in Fig. 11 for $n_1/n_2 = 1.005$. To obtain a performance for $n_1/n_2 = 1.005$ comparable to the case $n_1/n_2 = 1.01$ requires a higher-

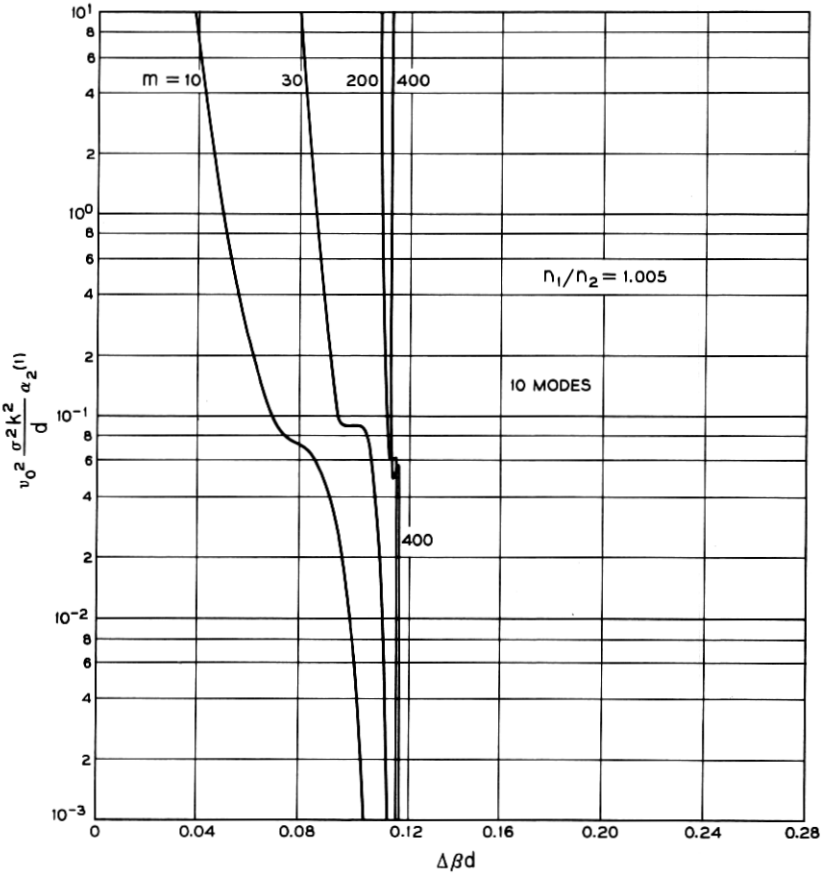

Fig. 11—The normalized second-order perturbation of the eigenvalue as a function of the width parameter of the "power spectrum" for the case $n_1/n_2 = 1.005$.

power m of the "power spectrum" curve (52) and a narrower spectrum.

The discussion of the loss penalty was based on the relative improvement factor R that determines how much the pulse is shortened compared to the pulse distortion in the absence of coupling. For an absolute comparison of pulse distortion it is important to keep in mind that the pulse distortion in the absence of coupling is less severe in a waveguide with smaller core-cladding index difference. Whereas we obtain

$$\frac{c}{n_1}\left(\frac{1}{v_N} - \frac{1}{v_1}\right) = 5.02 \times 10^{-3}$$

for the 10-mode case and $n_1/n_2 = 1.01$ (from Table II), we now have

$$\frac{c}{n_1}\left(\frac{1}{v_N} - \frac{1}{v_1}\right) = 1.94 \times 10^{-3}$$

for ten modes and $n_1/n_2 = 1.005$. The pulse distortion is already improved by a factor of 2.6 even in the absence of mode coupling simply by the reduction in the core-cladding index difference. The higher loss penalty that must now be paid for a given relative improvement R (provided we assume the same power factor m in both cases) is thus not quite as serious in absolute terms since the pulse distortion is already smaller for the smaller index difference.

VIII. APPLICATION TO ROUND OPTICAL FIBERS

Our discussion of numerical results of the pulse distortion reduction by means of coupling between guided modes was limited to the example of the slab waveguide. However, the slab waveguide results are meaningful for predicting the behavior of round optical fibers. In order to find the connection between round fibers and the slab waveguide let us use one intermediate step and consider a dielectric waveguide with square cross section. The behavior of dielectric waveguides with square cross section is very similar to the behavior of dielectric waveguides with circular cross section if the cross-sectional areas of the two waveguides are comparable. The modes of the slab waveguide can be visualized as plane waves (traveling in the core medium) that are reflected at the core-cladding interface. In the case of the slab waveguide we were concerned only with plane waves whose propagation vectors all lie in a plane that is positioned perpendicular to the core-cladding interface. The complete set of modes of the square waveguide is also made up of plane waves, except that now, for each plane wave propagating at a certain angle with respect to one parallel pair of interfaces, we have N waves whose propagation angle with one set of interfaces is fixed but whose angles with respect to the perpendicular set of interfaces are varying. Instead of the original N slab waveguide modes we find N^2 modes in the dielectric waveguide with square cross section. This discussion becomes more accurate with increasing values of N.

Turning now to the round optical fiber we can deduce from its similarity with the waveguide of square cross section that its total number of guided modes is also approximately given by N^2, where N is the number of slab waveguide modes. We assume that the slab half-width d corresponds approximately to the radius r of the round fiber. The 10-mode slab waveguide thus corresponds to a round optical fiber

supporting 100 guided modes. The largest number of modes considered in this paper, $N = 40$, thus corresponds to a round optical fiber supporting 1600 guided modes.

We assume that the coupling mechanism was caused by core-cladding interface irregularities of the slab waveguide with no variation in y direction. Extending our results to round optical fibers we consider a fiber with random core radius fluctuations with a carefully designed "power spectrum" but with no dependence of the core-cladding interface on the azimuth. Core radius variations of a round optical fiber couple only modes with the same azimuthal symmetry. This means that whole families of modes would remain uncoupled from each other. However, this defect does not prevent the pulse distortion reduction scheme from working. We must keep in mind that the modes within each family (all having the same azimuthal symmetry) cover the entire range in β space between n_2k and n_1k. The modes in each family would thus give rise to the spreading of the pulse described by (30). The random radius changes couple all the modes within each family reducing the spreading of the pulse to the amount given by (33). We thus can expect that instead of many pulses each traveling with its own group velocity, we now have families of pulses each traveling with an average velocity but each pulse being shortened by the coupling mechanism. Only if the pulses composed of each family of modes traveled with different average velocities would the pulse distortion reduction in the round fiber work less efficiently than predicted by our slab waveguide model. However, it can be expected that the average velocity of each pulse lies half way between the group velocities of the fastest and the slowest pulse in each family of modes. These average velocities must be very nearly the same. We thus expect that the pulse distortion reduction described in this paper is applicable to the round optical fiber. In designing the "power spectrum" of the random radius variation function, we must consider the spacing in β space between the modes of each family and must try to shape the "power spectrum" such that the guided modes within each family are coupled to each other with the exception of the highest-order mode whose strong coupling to the radiation field would cause excessive radiation losses. If this condition cannot be fulfilled for all mode families we may have to pay a higher loss penalty, losing certain families of modes more rapidly than others.

IX. CONCLUSIONS

We have found that pulse distortion resulting from the different group velocities of the many guided modes of a multimode waveguide

can be effectively reduced by providing coupling between the guided modes. We have seen, moreover, that we must be very careful to limit the coupling to those guided modes that are not coupled directly to the radiation field. Designing the power spectrum of the core-cladding interface irregularities responsible for the coupling mechanism in such a way, that the last guided mode becomes effectively uncoupled from the other guided modes, reduces radiation losses. The detailed discussion of the loss penalty that must be paid for a certain pulse distortion reduction showed that the slope of the core-cladding interface "power spectrum" must be extremely steep. Ideally, an infinitely steep slope would be desirable. The flat region of the power spectrum, shown in Figs. 3 and 5, is not a critical requirement. The delay distortion reduction would not be impaired if the power spectrum has ripples in this region.

In closing, it appears prudent to repeat the warning that our predictions are based on first-order perturbation theory. They hold only for weak coupling. For strong coupling the radiation losses are expected to be larger than predicted here. Furthermore, our theory predicts only average power values. Higher-order effects and the fluctuation problem will be discussed in future publications.

APPENDIX

The second-order perturbation theory is valid only provided that certain requirements are met. It is apparent from (18) that perturbation theory can be applied only if

$$\alpha_0^{(i)} \gg \omega^2 \alpha_2^{(i)} \tag{55}$$

with a suitably chosen value of ω. Instead of $\alpha_0^{(i)}$ and $\alpha_2^{(i)}$ the normalized quantities

$$\bar{\alpha}_0^{(i)} = \frac{d}{\sigma^2 k^2} \alpha_0^{(i)} \tag{56}$$

and

$$\bar{\alpha}_2^{(i)} = \frac{v_o^2 \sigma^2 k^2}{d} \alpha_2^{(i)} \tag{57}$$

are used for the actual numerical calculations. In terms of the numerical values used, (55) can thus be written as

$$\frac{v_o^2 \sigma^4 k^4}{\omega^2 d^2} \bar{\alpha}_0^{(i)} \gg \bar{\alpha}_2^{(i)}. \tag{58}$$

The effective value for ω to be used in these inequalities is related to the width τ of the input pulse,

$$\omega \approx \frac{1}{\tau}. \tag{59}$$

The required condition for the applicability of the perturbation theory is thus

$$\frac{v_o^2 \sigma^4 k^4 \tau^2}{d^2} \bar{\alpha}_0^{(i)} \gg \bar{\alpha}_2^{(i)}. \tag{60}$$

REFERENCES

1. Personick, S.D., "Time Dispersion in Dielectric Waveguides," B.S.T.J., *50*, No. 3 (March 1971), pp. 843–859.
2. Rowe, H. E., and Young, D. T., "Transmission Distortion in Multimode Random Waveguides," IEEE Transactions on Microwave Theory and Techniques, *MTT-20*, No. 6 (June 1972), pp. 349–365.
3. Marcuse, D., "Derivation of Coupled Power Equations," B.S.T.J., *51*, No. 1 (January 1972), pp. 229–237.
4. Marcuse, D., "Mode Conversion Caused by Surface Imperfections of a Dielectric Slab Waveguide," B.S.T.J., *48*, No. 10 (December 1969), pp. 3187–3215.
5. Marcuse, D., *Light Transmission Optics*, New York: Van Nostrand Reinhold Comp., 1972.
6. Marcuse, D., "Radiation Losses of Waveguides in Terms of Power Spectrum of the Wall Distortion Function," B.S.T.J., *48*, No. 10 (December 1969), pp. 3233–3242.
7. Marcuse, D., "Power Distribution and Radiation Losses in Multimode Dielectric Slab Waveguides," B.S.T.J., *51*, No. 2 (February 1972), pp. 429–454.